Importance of energy band theory and screening charge effect in piezo-electrocatalytical processes

Electrochimica Acta 462 (2023) 142730

Contents lists available at ScienceDirect

Electrochimica Acta

journal homepage: www.journals.elsevier.com/electrochimica-acta

Importance of energy band theory and screening charge effect in piezo-electrocatalytical processes

Franziska Bößl [a,*], Valentin C. Menzel [a], Karina Jeronimo [b], Ayushi Arora [c], Yishu Zhang [c], Tim P. Comyn [d], Peter Cowin [d], Caroline Kirk [c], Neil Robertson [c], Ignacio Tudela [a,1,*]

[a] School of Engineering, Institute for Materials and Processes, Edinburgh Electrochemical Engineering Group (e3 Group), The University of Edinburgh, Sanderson Building, Robert Stevenson road, Edinburgh EH9 3FB, UK
[b] School of Engineering, Institute for Integrated Micro and Nano systems, Scottish Microelectronics Centre, University of Edinburgh, Alexander Crum Brown Road, Edinburgh EH9 3FF, UK
[c] School of Chemistry, The University of Edinburgh, Joseph Black Building, David Brewster road, Edinburgh EH9 3FJ, UK
[d] Ionix Advanced Technologies Ltd., 3 M Buckley Innovation Centre, Firth Street, Huddersfield HD1 3BD, UK

ARTICLE INFO

Keywords:
Piezo-electrocatalysis
Piezocatalysis
Energy band theory
Screen charge effect
Sonocatalysis
Sonochemistry

ABSTRACT

The present study tries to shed more light on the controversial discussion around the 'true' mechanism behind piezo-electrocatalysis: energy band theory or screening charge effects. For this purpose, piezo-electrocatalysts made of three different materials with different energy band levels and piezoelectric properties, ZnO, $BaTiO_3$ and BF-KBT-PT, were used to degrade Rhodamine B in aqueous solutions where combined ultrasound and mechanical agitation was used as the excitation method. The results suggest that both mechanisms may actually play an important role in the overall process, as the largest overall dye degradation was achieved with the piezo-electrocatalyst most likely to generate radicals via both piezo-electrocatalytic mechanisms.

1. Introduction

Over the last decade, a new concept known as *piezocatalysis* [1–5], *piezo-electrocatalysis* [6–10] or *piezo-electrochemistry* [11–16] has attracted a wide attention of the catalysis community. Piezo-electrocatalysis is based on the occurrence of redox reactions at the surface of a piezoelectric material driven by its polarisation under applied mechanical stress. To some extent, it could be considered that piezo-electrocatalysts behave as miniaturised electrochemical devices that combine a power source and electrodes. Due to this advantage and the long-term aim to harness redundant mechanical vibrations in industrial systems [5], piezo-electrocatalysis is seen as an intriguing concept with the potential to drive electrochemical reactions without the use of more traditional energy sources such as light and electricity.

However, despite the rising numbers of reports exploring piezo-electrocatalysis (mostly focused on the development of novel piezo-electrocatalyst materials), the mechanism behind the reported catalytic activity remains controversial. Over the years, the research community has proposed two main potential mechanisms, i.e. screening charge effect and energy band theory, and the way the academic debate has developed over time is that either one *or* the other is the 'true' mechanism behind piezo-electrocatalysis [2].

The screening charge effect mechanism implies that redox reactions over the surface of piezo-electrocatalysts rely entirely on the piezoelectric polarisation generated by the deformation of the piezo-electrocatalyst [1,4,14,17,18]. In this mechanism, the piezoelectric potential experienced by the piezo-electrocatalyst should exceed the difference between the reduction potentials of the redox reactions of interest. In other words, the piezoelectric potential will determine its ability to drive specific electrochemical reactions in certain regions of the surface, which would act as either cathode or anode. This screening charge effect mechanism has recently moved away from 'bulk' piezoelectric polarisation towards a more localised piezoelectric response [19–24]. Under ultrasound, asymmetrical collapse of cavitating bubbles near the piezo-electrocatalyst [25], amongst other mechanical effects caused by cavitation, would lead to localised high pressures of several hundreds of bars [26] that could result in superficial piezoelectric polarisation of micro- and nano-features of the catalysts [19–25,27,28].

The energy band mechanism is analogous to photocatalysis where redox reactions, which take place over the surface of piezo-

* Corresponding authors.
E-mail addresses: f.boessl@ed.ac.uk (F. Bößl), ignacio.tudela@ed.ac.uk (I. Tudela).
[1] ISE member

https://doi.org/10.1016/j.electacta.2023.142730
Received 12 March 2023; Received in revised form 19 May 2023; Accepted 10 June 2023
Available online 16 June 2023

electrocatalysts, are determined by the energy band levels of the valence and conduction bands [3,29–31]. Based on this theory, the piezoelectric polarisation of the piezo-electrocatalyst is considered an indirect promoter of electrochemical reactions by adjusting the band structure and controlling internal charge flow to the surface of the piezo-electrocatalyst [2]. If energy band theory was the dominant mechanism behind piezo-electrocatalysis, one would expect superior piezo-electrocatalytic performance when using a piezo-electrocatalyst having a wide enough energy band gap to drive targeted electrochemical reactions. The electrochemical potential derived from the excitation of electrons to higher energy levels must not only be sufficient for those redox reactions to occur, but also should be enough to overcome kinetic and concentration overpotentials, as well as ohmic losses. Further to this, the band configuration and electronic states of the piezo-electrocatalyst have to be appropriate for the reduction and oxidation reactions of interest to occur.

The preliminary study presented here followed a simple approach to explore the importance of energy band theory and screening charge effect in piezo-electrocatalysis by investigating the performance of different piezo-electrocatalysts on the degradation of Rhodamine B (RhB) under combined ultrasound and mechanical agitation. The piezo-electrocatalysts consisted of three different piezoelectric materials, allowing for the two mechanisms to be studied in isolation and combination through the different energy band levels and piezoelectric characteristics of these materials:

- Zinc oxide (ZnO) was chosen due to its wide energy band gap [32–34] and weaker piezoelectric performance [35–38] in comparison with the properties of the other piezo-electrocatalysts used in this study. For this material, any piezo-electrocatalytic effect on the overall degradation of RhB would most likely occur in accordance to the energy band mechanism rather than the screening charge effect.
- Potassium bismuth titanate-bismuth ferrite lead titanate (BF-KBT-PT) was chosen due to its very high piezoelectric properties [27,39,40] and narrow energy band gap. This implied that any piezo-electrocatalytic contribution to the overall degradation of RhB would be solely caused by the screening charge mechanism.
- Barium titanate ($BaTiO_3$) was chosen due to its combination of very high piezoelectric properties and a wide energy band gap [4,41–44]. This would make $BaTiO_3$ an interesting option, as it could potentially benefit from both mechanisms simultaneously; higher piezo-electric contribution towards the degradation of RhB would therefore be expected from this piezo-electrocatalyst.

In the case of BF-KBT-PT and $BaTiO_3$, the performance of both poled (highly piezoelectric) and unpoled (non-piezoelectric) versions of the same materials were investigated to get a better picture of the importance of the piezoelectric nature in the overall performance of the piezo-electrocatalysts.

2. Experimental

2.1. Catalyst preparation and characterisation

2.1.1. Catalysts preparation

ZnO nanoflowers were synthesised via a hydrothermal method previously described by the authors [38]. Equimolar concentrations (20 mM) of $Zn(NO_3)_2{\cdot}6H_2O$ and hexamethylenetetramine were added to de-ionized water and magnetically stirred for 10 min. The solution was then sealed and kept in an oven at 90 °C for 18 h. The resulting solution was cooled down to room temperature, washed and centrifuged three times with ethanol. The remaining white sediment in ethanol (i.e. ZnO nanoflowers) was left to dry at room temperature overnight.

Commercial $BaTiO_3$ piezoceramic discs (Steiner & Martins, Inc.) with high piezoelectric properties (d_{33} and d_{31} values of 160 pC/N and 30 pC/N, respectively, measured according to IEEE standards [45,46]) were used to fabricate P and UP versions of the $BaTiO_3$ piezo-electrocatalysts. The $BaTiO_3$ piezoceramic discs (i.e. poled materials with aligned ferroelectric domains) were ground into fine particles (<63 μm) following the method described by the authors in a previous study [27], to fabricate the P $BaTiO_3$ piezo-electrocatalysts. To obtain the unpoled version (non-piezoelectric; d_{33} and d_{31} values of 0 pC/N) of this material, the commercial $BaTiO_3$ piezoceramics were depoled by heating them above their Curie temperature for several hours and cooling them down to room temperature to produce UP $BaTiO_3$ piezo-electrocatalysts (i.e. unpoled materials with randomly orientated ferroelectric domains).

ZnO and both P and UP $BaTiO_3$ piezo-electrocatalysts were compared with P and UP BF-KBT-PT piezo-electrocatalysts already evaluated under the same experimental conditions in a previous study by the authors [27], except for their energy band information. P and UP BF-KBT-PT piezo-electrocatalysts had been prepared from poled and depoled piezoceramic discs of the same material, with the poled discs exhibiting a strong piezoelectric behaviour (d_{33} and d_{31} values of 100 pC/N and −40 pC/N, respectively) while the unpoled discs exhibited no piezoelectricity at all (d_{33} and d_{31} values of 0 pC/N) [27].These discs were also ground into fine particles (<63 μm) to fabricate P and UP BF-KBT-PT piezo-electrocatalysts.

2.1.2. Catalyst characterisation

The morphology, surface structure and composition of all piezo-electrocatalysts was analysed using a focused ion beam-scanning electron microscopy (FIB-SEM, Zeiss Gemini 2 crossbeam 550) equipped with an energy dispersive X-ray spectrometer (EDS). X-ray powder diffraction (XRPD) data for all piezo-electrocatalysits was obtained with a Bruker D2 PHASER diffractometer equipped with Cu Kα radiation to confirm the identity of the crystalline phases of the materials. Data were collected over the 2θ range from 5 to 60° and a scanning speed of 0.2 steps/second. Energy band gaps were determined by ultraviolet–visible diffuse reflectance spectroscopy (UV–Vis DRS) using a JASCO V-670 spectrophotometer equipped with an integrating sphere attachment. Direct and indirect band gaps were quantified using Kubleka-Munk theory and corresponding Tauc plots. The valence band maximum of all the materials used in this study was estimated by X-ray photoelectron spectrometry (XPS) in a Scienta XPS system equipped with monochromatic source.

2.2. Experimental setups and procedures

RhB degradation experiments were conducted under the same conditions defined in a previous study by the authors [27], where combined ultrasound and mechanical agitation was used as the mean to excite the piezo-electrocatalysts. For this purpose, a SciQuip Basic 20 overhead stirrer was centred and immersed into a 1000 mL beaker acting as the reactor; the beaker was also centred and immersed to a 4 cm depth into a 32–38 kHz Ultrawave QS12 ultrasonic bath with constant water level. At full ultrasonic power and mechanical agitation of 200 rpm, the experimental setup was calibrated by calorimetry [47], resulting in a dissipated acoustic power of 14.3 ± 0.7 W L^{-1}. Prior to each experiment, the water in the ultrasonic bath was thoroughly degassed for 60 min to ensure a reproducible acoustic field inside the bath. The temperature in the reactor was kept at 30 ± 2 °C throughout all the experiments by a precise temperature control system (Grant LT ecocool 100 recirculating chiller).

120 min control (i.e. no piezo-electrocatalyst) and piezo-electrocatalytic RhB degradation experiment were performed on 1000 mL of 5 mg L^{-1} aqueous solutions at pH = 4.5. In each experiment, 3-mL aliquots of the RhB solution were sampled every 10 min with a 0.22 μm PTFE-syringe-filter. In the particular case of ZnO piezo-electrocatalysts, samples were also centrifuged to remove the nanoflowers from the solution. Ultraviolet–visible spectroscopy at the characteristic wavelength of 554 cm was conducted in a Shimadzu UV-3600 Plus spectrophotometer to analyse the solution samples. In all piezo-

electrocatalytic experiments, 1 g L^{-1} of piezo-electrocatalysts were added to the RhB solutions to be treated. Prior to each experiment, though, adsorption-desorption equilibrium was ensured by mechanically stirring the catalysts at 200 rpm for 30 min in the RhB solution (no RhB adsorption was observed in all cases).

3. Results and discussion

3.1. Piezo-electrocatalyst characterisation

FIB-SEM and EDS analysis provided interesting details on the morphology and surface structure of the piezo-electrocatalysts used in this study, and confirmed the composition of the different materials used. The ZnO piezo-electrocatalysts generally presented a flower-like structure formed by nanorods growing radially from the centre of the particles (Fig. 1a, left). As expected from previous work [38], the individual nanorods were several microns long with an average length ranging from 3 to 6 μm, and a diameter of several hundreds of nanometers with an average diameter around 180–220 nm (Fig. 1a, centre). EDS confirmed that the ZnO piezo-electrocatalysts were free from any impurities (Fig. 1a, right). P and UP BF-KBT-PT piezo-electrocatalysts presented identical cuboid morphology with sizes of the order of several tens of microns (Fig. 1b and c, left) where smaller debris originating from the catalyst fabrication process (i.e. grinding of piezoceramic discs) could be noticed over the surface (Fig. 1b and c, centre); both versions of BF-KBT-PT also presented identical composition (Fig. 1b and c, right).

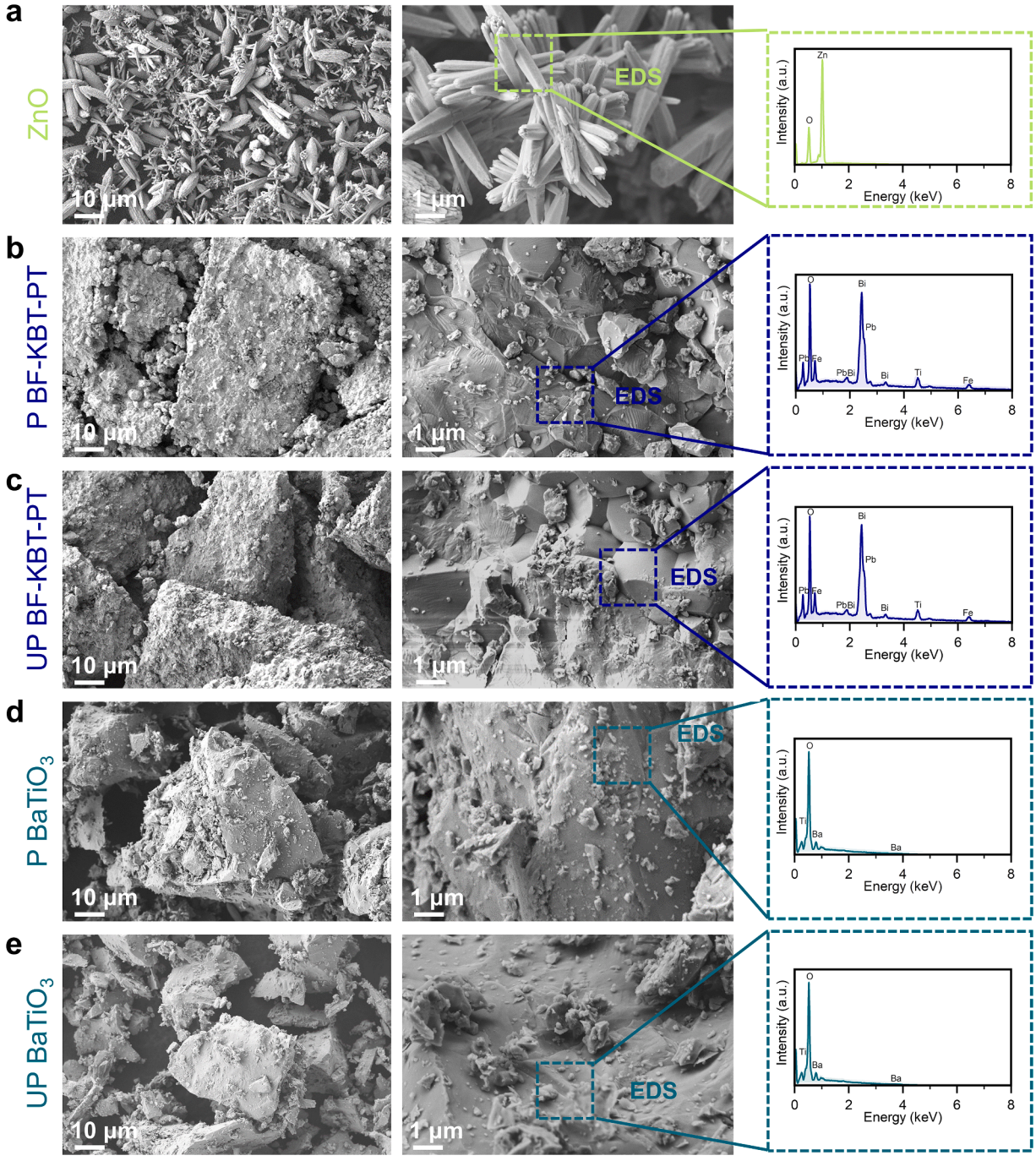

Fig. 1. FIB-SEM and EDS analysis of the different piezo-electrocatalysts used in this study: (a) ZnO, (b) P BF-KBT-PT, (c) UP BF-KBT-BT, (d) P $BaTiO_3$, and (e) P $BaTiO_3$.

This confirmed that, in terms of shape, surface structure and composition, P and UP BF-KBT-PT piezo-electrocatalysts were virtually the same material. The same trend was confirmed for P and UP $BaTiO_3$ piezo-electrocatalysts, which also presented a cuboid morphology with sizes of the same order of several tens of microns (Fig. 1d and e, left) where smaller debris were again noticed over the surface (Fig. 1d and e, centre); no difference was observed in terms of material composition between the P and UP piezo-electrocatalysts (Fig.1d and e, right).

XRPD analysis was used to confirm the phase(s) present in the piezo-electrocatalysts used in this study (Fig. 2). XRPD data collected on the ZnO sample matched well to the standard International Centre for Diffraction Data (ICDD) Powder Diffraction File (PDF) [36–1451], confirming the piezo-electrocatalyst sample was the hexagonal wurtzite polymorph of ZnO. The three main characteristic peaks observed at 32°, 34° and 36° were clearly identified, confirming good crystallinity of the prepared ZnO piezo-electrocatalysts. XRPD data of both P and UP BF KBT-PT piezo-electrocatalysts indicated phase co-existence due to peak splitting in most of the reflections [39], especially in the case of the (110) planes, as reported before by the authors [27,39]. Lattice distortion of the rhombohedral phase was considered negligible due to no observed peak splitting in of the 111 reflection and only minor peak splitting of the 200 reflection, which is characteristic of tetragonal materials [39]. Minor differences in signal intensities were observed for the P and UP BF-KBT-PT piezo-electrocatalysts were noticed. However, the relative heights of both samples were the same for both versions of BF-KBT-PT, confirming their identical phase structure. The XRPD data collected on the P and UP $BaTiO_3$ piezo-electrocatalyst samples matched well to the standard International Centre for Diffraction Data (ICDD) Powder Diffraction File (PDF) [74–1959] for tetragonal $BaTiO_3$. Both P and UP $BaTiO_3$ piezo-electrocatalysts showed the presence of only the perovskite $BaTiO_3$ phase, with no other peaks observed showing no impurity phases were present. Peak splitting was observed in both the P and UP $BaTiO_3$ at around 45°, where the 200 peak in the cubic polymorph splits into (002) and (200), indicating the tetragonal polymorph of $BaTiO_3$ is present [1,48].

The Kubelka-Munk function was applied to collected UV–Vis DRS data (Fig. 3a) to produce Tauc plots that allowed the energy band gaps of all piezo-electrocatalysts to be estimated: ZnO (Fig. 3b), P versions of BF-KBT-PT and $BaTiO_3$ (Fig. 3c), and UP versions of BF-KBT-PT and $BaTiO_3$ (Fig. 3d). The value of the band gap for ZnO was quite high (3.20 eV), as expected from the literature [33,34]. Similar band gaps values (3.18 eV) were obtained for P and UP $BaTiO_3$, which were also in agreement with values from the literature [41,42], confirming that the energy band gap value did not depend on whether the piezo-electrocatalyst was poled or unpoled. The same trend was observed for the P and UP BF-KBT-PT piezo-electrocatalysts, although in this case, both versions of this material exhibited a significantly lower energy band gap (2.16 eV) than the other materials studied in this work. XPS data was used to estimate values of the valence band edge for all piezo-electrocatalysts used in this study (Fig. 3e). The values of the valence band edge for both P and UP versions of the same material (either BF-KBT-PT or $BaTiO_3$) were nearly identical, as was the case for the energy band gap levels.

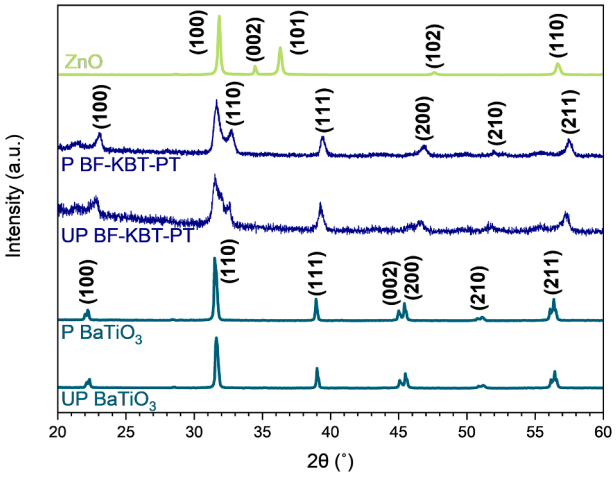

Fig. 2. XRPD data collected on the different piezo-electrocatalysts used in this study: ZnO, P and UP BF-KBT-PT, and P and UP $BaTiO_3$.

Valence band edge values obtained from XPS data were used to estimate the valence band maximum (VBM) vs SHE (Standard Hydrogen Electrode) of all the piezo-electrocatalysts after taking into account the electronic energy of SHE (−4.44 eV) [49] and the work function of the XPS system (4.5 eV). VBM values were then used, along with the band gap values obtained from the application of the Kubelka-Munk function to the UV–Vis DRS data, to estimate the conduction band minimum (CBM) vs SHE for all the piezo-electrocatalysts. VBM and CBM values were also used to construct the band alignment diagram for all the piezo-electrocatalysts used in the present study (Fig. 4). The standard equilibrium potential of those redox reactions responsible for the generation of superoxide ($^{\bullet}O_2^-$) and hydroxyl ($^{\bullet}OH$) radicals at the surface of piezo-electrocatalyst [1,13], which are responsible for the degradation of RhB [25,27], were also included in the diagram, along with the equilibrium potential for the hydrogen evolution reaction (HER) and oxygen evolution reaction (OER) at pH = 4.5 (i.e. the pH of the RhB solutions used in this study):

- Reduction reactions
  - $O_2 + e^- \leftrightarrow {}^{\bullet}O_2^-$ (−0.33 V vs SHE) [50]
  - $2\,H^+ + 2\,e^- \leftrightarrow H_2$ (−0.27 V vs SHE)
- Oxidation reactions
  - $OH^- + h^+ \leftrightarrow {}^{\bullet}OH$ (1.89 V vs SHE) [51]
  - $2\,H_2O \leftrightarrow O_2 + 4\,H+ + 4\,e^-$ (0.96 V vs SHE)

It should be noted that, as the VBM values were obtained from XPS measurements, they are intrinsically true under vacuum. However, that may not be fully representative of the 'real' conditions in the experiments (i.e. RhB solution at pH = 4.5). Ideally, Mott-Schottky plots obtained for electrodes fabricated with the catalysts (e.g. by drop casting) and immersed in the working solution should be used to estimate the flatband potential, which could then be considered as the conduction band in the case of an n-type semiconductor or the valence band in the case of a p-type semiconductor. This was not an option in this study due to the nature of most of the piezo-electrocatalysts used in the study (i.e. P and UP versions of both $BaTiO_3$ and BF-KBT-PT had a size of several tens of microns and a cuboid shape), which made it impossible to prepare electrodes with smooth and uniform surfaces where full coverage of the substrate was achieved. Nevertheless, in the case of the P and UP $BaTiO_3$ piezo-electrocatalysts, if it is considered that the isoelectric point of diluted suspensions of $BaTiO_3$ in deionised water is reached at pH ≈ 6.5 [52], it is reasonable to believe that the bandgaps depicted for both piezo-electrocatalysts in Fig. 4 would be, to some extent, displaced to more positive potentials in the experimental conditions used here. The ZnO piezo-electrocatalysts would be in a similar situation, provided that the isoelectric point of ZnO nanoparticles in water is reached at pH ≈ 10.3 [53]. The case of P and UP BF-KBT-PT piezo-electrocatalysts is slightly more complex, given that it is a ternary system ($BiFeO_3$, $K_{0.5}Bi_{0.5}TiO_3$ and $PbTiO_3$) [39]. Whereas the isoelectric point for $BiFeO_3$ is reached at pH ≈ 2.8 [54], the isoelectric point of $PbTiO_3$ is reached at pH ≈ 11.5 [55]; however, no isoelectric point data is available for $K_{0.5}Bi_{0.5}TiO_3$. Therefore, it was deemed reasonable to assume that the bandgaps depicted for both P and UP BF-KBT-PT piezo-electrocatalysts in Fig. 4 would not be significantly displaced to either more positive or negative potentials.

3.2. Reaction mechanisms

The material characterisation previously included confirmed that P

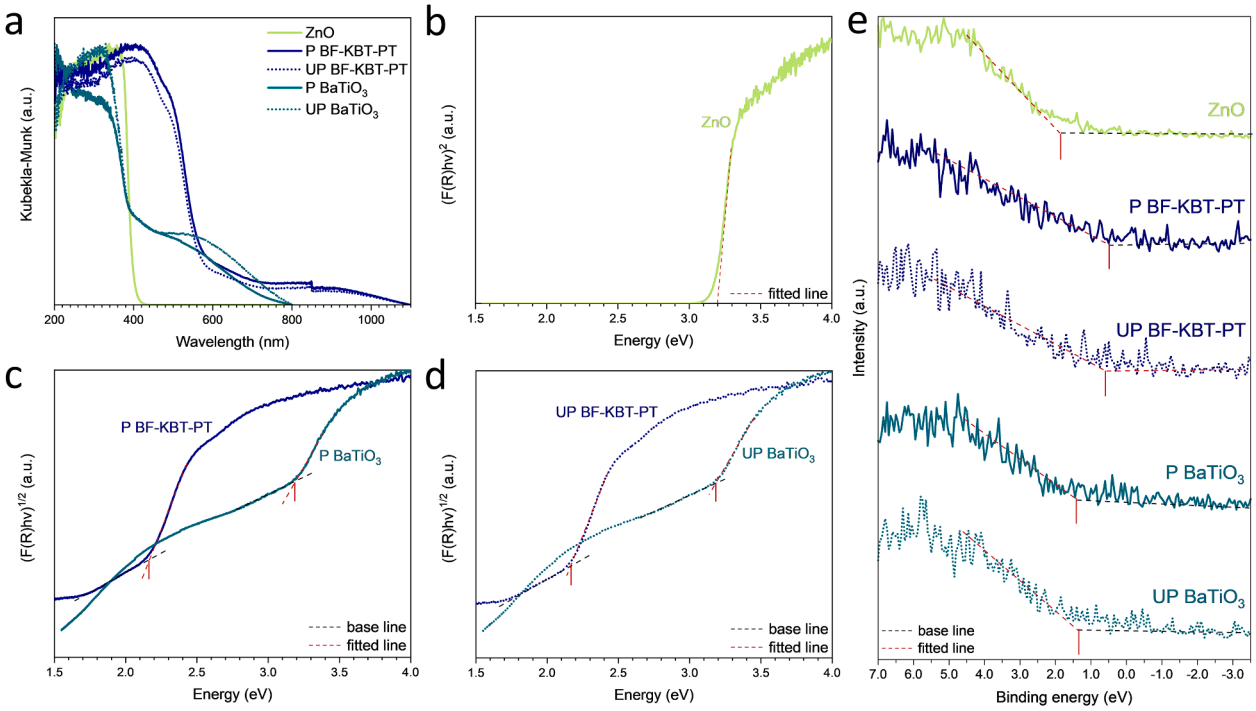

Fig. 3. (a) Application of Kubelka-Munk to UV–Vis DRS data, (b–d) corresponding Tauc plots, and (e) XPS data collected on all piezo-electrocatalysts used in this study: ZnO, P and UP BF-KBT-PT, and P and UP $BaTiO_3$.

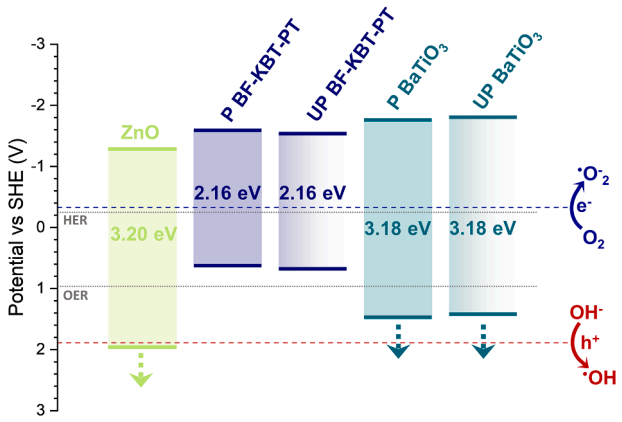

Fig. 4. Band alignment diagram for all piezo-electrocatalysts used in this study: ZnO, P and UP BF-KBT-PT, and P and UP $BaTiO_3$. Arrows indicate direction of the displacement of bandgaps in RhB degradation experiments.

and UP $BaTiO_3$, as well as P and UP BF-KBT-PT, were virtually identical except for their poled or unpoled nature. The knowledge of the piezoelectric nature of all piezo-electric materials used in this study, along with their energy band levels, would already give a strong indication of which reaction mechanisms are likely to occur for each piezo-electrocatalyst, and which one is likely to deliver the highest piezo-electrocatalytic contribution towards the overall degradation of RhB. To discuss this, though, the possible piezo-electrocatalytic mechanisms that could be taking place must also be further explained at the same time (Fig. 5).

The screening charge mechanism [2] would be based on the localised superficial piezoelectric response of micro- and nano-scale features of the surface of piezo-electrocatalysts [28] under periodic mechanical stress (Fig. 5a), which would be caused in this case by acoustic cavitation (i.e. asymmetrical bubble collapse near to the surface) [25]. Without any applied external force, the surfaces of poled piezo-electrocatalysts remain electrically neutral as bound charges are balanced by screening charges from the electrolyte [56] (e.g. charged adsorbates) [57]. However, under a mechanical strain (e.g. that resulting from the acoustic cavitation phenomena caused by ultrasound), the charge balance is disrupted, leading to a redistribution of bound charges where electrons and holes travel to different surfaces of the piezo-electrocatalyst, which become oppositely polarised. As a result, more screening charges of opposite sign in the electrolyte will be attracted and adsorbed onto the polarised surfaces, balancing again the bound charges in those surfaces. Once the mechanical strain becomes weaker, bound charges will start to leave those polarised surfaces, which will obviously become less polarised, resulting in an excess of screening charges. This excess of screening charges would then be released from the surface until a charge balance in those surfaces is reached again; these charges could then take part in redox reactions with the surrounding electrolyte near the piezo-electrocatalyst surface. These same steps would then occur again and again in a cyclic way as the piezo-electrocatalysts are subject to ultrasound and the action of acoustic cavitation and its mechanical effects. Worth noting here is that screening charges may be sourced from many sources such as electrons, holes, anions and cations, cationic vacancies and polar molecules, indicating that there is still much research to do in order to identify how this could affect this mechanism [2]. In any case, it is obvious that the piezoelectric properties of the material will be important for this mechanism to make a greater impact on the degradation of RhB, which is why P versions of the materials with high piezoelectric properties (i.e. BF-KBT-PT and $BaTiO_3$) would be more likely to experience this mechanism. Nevertheless, localised piezoelectric polarisation at the domain level could be enough for piezo-electrocatalytical processes to occur at the surface of non-piezoelectric ferroelectric materials [20]. This also means that, as well as ZnO (which is significantly less piezoelectric than P BF-KBT-PT and $BaTiO_3$), UP versions of the BF-KBT-PT and $BaTiO_3$ piezo-electrocatalysts could also experience enough localised piezoelectric activity to drive those same redox reactions, but in a lesser extent.

The mechanism based on energy band theory is strongly related to

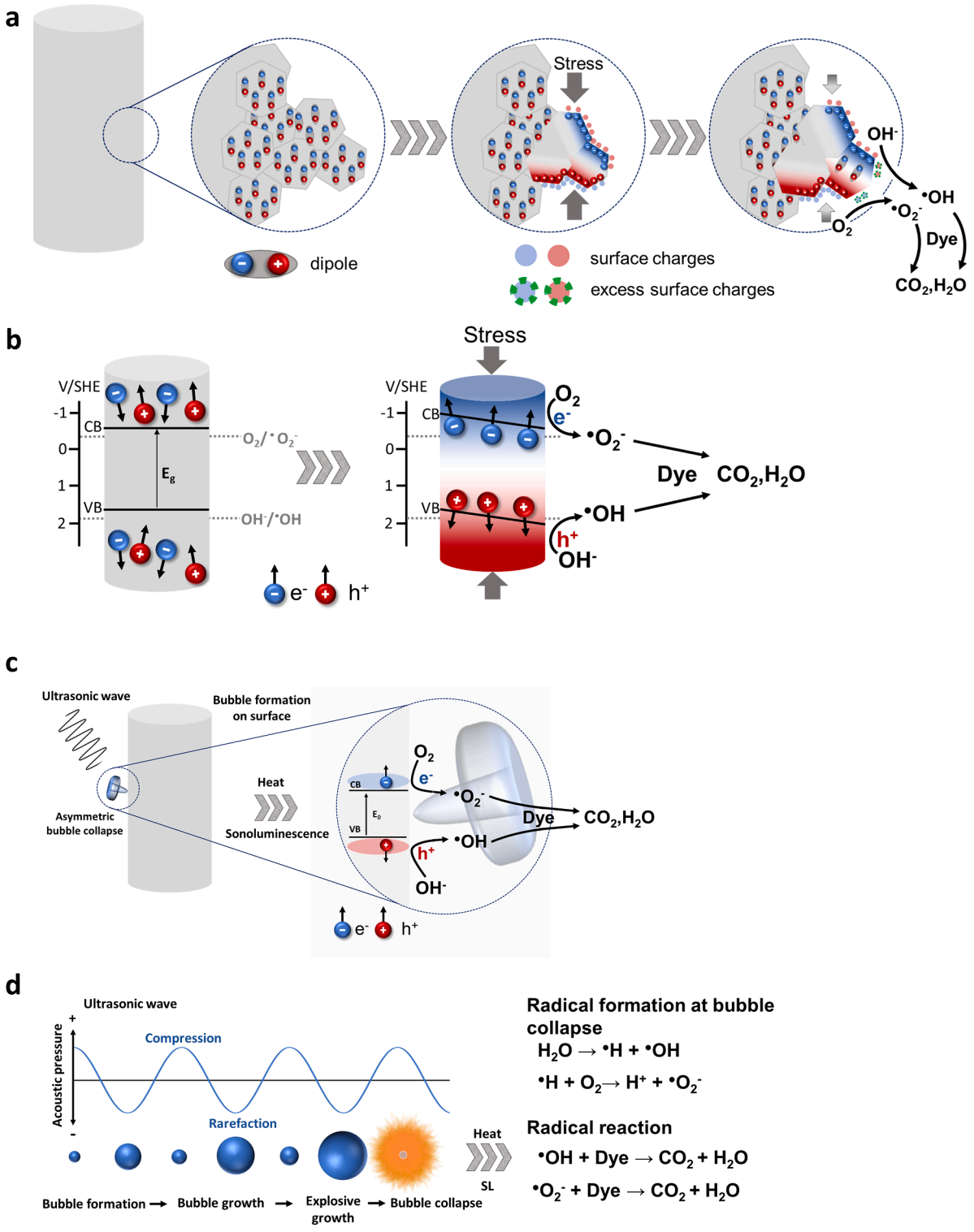

Fig. 5. Illustration of different mechanisms for overall dye degradation: (a) Screening charge effects via localised piezoelectric response, (b) Energy band theory mechanism, (c) Sonocatalytic mechanisms, (d) Sonochemical mechanism.

photocatalysis, as electrons would be excited from the valence band (VB) to the conduction band (CB), leading to the generation of reactive species (i.e. electrons and holes) driving redox reactions. However, in piezo-electrocatalysis, this excitation would rely on mechanical energy rather than light. It is still under debate whether this excitation is a result of direct excitation due to the high pressures of collapsing bubbles or a thermally induced indirect excitation [2]. In any case, the piezopotential generated within the piezoelectric material would lead to an improvement in the redox capability of the piezo-electrocatysts due to the bending/tilting of the energy bands (Fig. 5b). This would enable the alignment of the valence and conduction bands over/under the equilibrium potentials of the anodic/cathodic redox reactions of interest [2], which in this case are those involved in the generation of superoxide and hydroxyl radicals (Fig. 4). Obviously, this means that those materials highly piezoelectric in nature, which also exhibit wide band gaps and suitable VBM and CBM values likely to be bended/tilted beyond the

equilibrium potentials, would be likely to induce the generation of radicals via the energy band mechanism. In the present study, P $BaTiO_3$ piezo-electrocatalysts would be very likely to degrade RhB via superoxide and hydroxyl radicals generated by this mechanism due to their wide bang gap and VBM relatively close to the potential required to generate hydroxyl radicals. In a first instance, ZnO might also seem in a very strong position to also experience this due to its energy band levels. However, the degradation should not be as high as one might initially expect due to its relative poor piezoelectric nature. In the case of P BF-KBT-PT piezo-electrocatalysts, their band gap is rather narrow, and although their CBM would enable the generation of superoxide radicals, the generation of hydroxyl radicals via this mechanism would be highly unlikely due to their VBM, despite their strong piezoelectric nature. A similar situation would be expected for the UP versions of BF-KBT-PT and $BaTiO_3$, with the addition that these piezo-electrocatalysts are not intrinsically piezoelectric; therefore, no superoxide and hydroxyl radicals should be generated by the energy band mechanism.

Besides the piezo-electrocatalytic mechanisms just discussed (based on the screening charge effect and energy band theory), there is another potential mechanism that must always be considered whenever semiconductors such as the piezoelectric materials used in this study are suspended in a liquid solution irradiated with ultrasound: sonocatalysis (Fig. 5b). Sonocatalysis is even more similar to photocatalysis, where the excitation of the electrons would be caused either thermally or by sonoluminescence due to the action of cavitating bubbles collapsing nearby the surface of the material [58]. The band alignment diagram (Fig. 4) again indicates that the generation of superoxide radicals via sonocatalysis would be likely to occur in all of the materials studied here. However, the generation of hydroxyl radicals should only take place sonocatalytically in the ZnO piezo-electrocatalysts, and not on the other materials.

The previous paragraphs can be summarise as follows:

- In the case of ZnO piezo-electrocatalysts, it would be expected that, based on its energy band characteristics and piezoelectric properties, both superoxide and hydroxyl radicals were generated by piezo-electrocatalysis via the energy band and screening charge mechanisms, as well as sonocatalytically. However, both piezo-electrocatalytical mechanisms would be limited due to the material's relatively poor piezoelectric nature, which is why sonocatalysis may be the predominant mechanism in this case [59]. Although it is already well known that ZnO piezo-electrocatalysts suspended in aqueous solutions under ultrasound generate superoxide radicals, hydroxyl radicals and holes [60,61], it is expected that the contribution of ZnO piezo-electrocatalysts to the overall degradation of RhB may not be the greatest of all the piezo-electrocatalysts used in this study.
- In the case of P $BaTiO_3$, its energy band levels and highly piezoelectric nature should result in significant generation of superoxide and hydroxyl radicals via both piezo-electrocatalytical mechanisms, which would obviously enhance the overall degradation of RhB; many studies have indeed confirmed the generation of superoxide radicals, hydroxyl radicals and holes under ultrasound with this material [62–64]. Whereas superoxide radicals could also be generated via sonocatalysis, this would not be the case for the generation of hydroxyl ions.
- In the case of P BF-KBT-PT piezo-electrocatalysts, whereas superoxide radicals could also be generated via the sonocatalytical and both piezo-electrocatalytical mechanisms, the hydroxyl radical could only be generated via the piezo-electrocatalytical screening charge mechanism due to its energy band alignment. The authors already demonstrated the capability of P BF-KBT-PT to generate superoxide radicals, hydroxyl radicals and holes, as well as their critical role on the degradation of RhB, under identical conditions [25,27]; however, it would be expected, that its performance would be lower than that of P $BaTiO_3$ piezo-electrocatalysts as the latter could also benefit from the piezo-electrocatalytic energy band mechanism.
- The UP versions of the BF-KBT-PT and $BaTiO_3$ should exhibit lower catalytic effect than their P counterparts due to their non-piezoelectric nature. For this reason, if any piezo-electrocatalytic degradation of RhB was observed with these materials, it would most likely be caused by localised screen charge effect at the domain level.

It should be noted, however, that there is an additional mechanism for the formation of the superoxide and hydroxyl radicals [25] involved in the degradation of RhB, which does not require the presence of any catalyst. That mechanism is based on sonochemistry (Fig. 5d), where the production of radicals is driven by the extreme high temperatures (order of 5000 K) and pressures (order of 1000 atm) reached at the centre of cavitating bubbles after their collapse once they have reached a certain size [65]. This mechanism is therefore expected to play a significant role in the overall degradation of RhB under the experimental conditions of this study, as already demonstrated in the past by the authors [27].

3.3. Degradation experiments

Fig. 6 displays the normalised concentration of RhB during different degradation experiments conducted under combined ultrasound and mechanical stirring, in the absence (MA + US; i.e. sonochemical degradation own its own) and presence of the ZnO, BF-KBT-PT and $BaTiO_3$ piezoelectro-catalysts (both P and UP versions in the case of BF-KBT-PT and $BaTiO_3$). First order kinetics derived from Langmuir-Hinshelwood theory were used to estimate the overall degradation reaction rates in absence and presence of the different piezo-electrocatalysts:

$$\frac{C}{C_0} = e^{-kt} \tag{1}$$

where t was time, C was the concentration of RhB at time t, C_0 was the initial concentration of RhB and k was the kinetic degradation rate constant. The overall degradation efficiency (DE) was calculated using the following expression:

$$DE = \left(1 - \frac{C}{C_0}\right) \times 100 \tag{2}$$

As expected, significant degradation of RhB was already achieved in absence of a piezo-electrocatalyst (MA + US) via sonochemistry on its own (DE = 50% after 60 min). The addition of the UP versions of BF-KBT-PT and $BaTiO_3$ piezo-electrocatalysts resulted in a relatively small enhancement of the degradation of RhB (DE values of 54% and 61%, respectively); this enhancement would mostly rely on the piezo-electrocatalytic screening charge mechanism, as discussed in the previous section. The P versions of the same materials, P BF-KBT-PT and P $BaTiO_3$, delivered a further enhancement of the degradation of RhB. In the case of P BF-KBT-PT, there was a relative improvement of 22% compared to sonochemistry on its own (DE = 61%). This indicates that, even though the piezo-electrocatalytic screening charge mechanism would be taking place in the presence of both UP and P versions of BF-KBT-PT, this mechanism was significantly enhanced by the highly piezoelectric nature of P BF-KBT-PT, highlighting the importance of the piezoelectric properties of the material in piezo-electrocatalysis. This was even more remarkable in the case of P $BaTiO_3$, where an outstanding improvement of 50% was achieved compared to sonochemistry on its own (DE = 73%). In this case, however, this improvement would not be caused by the piezo-electrocatalytic screening charge mechanism on its own, but also by the piezo-electrocatalytic energy band mechanism, as discussed in the previous section. This indicates that developing piezo-electrocatalysts highly piezoelectric in nature *with* suitable energy band alignments should be the aim, as both piezo-

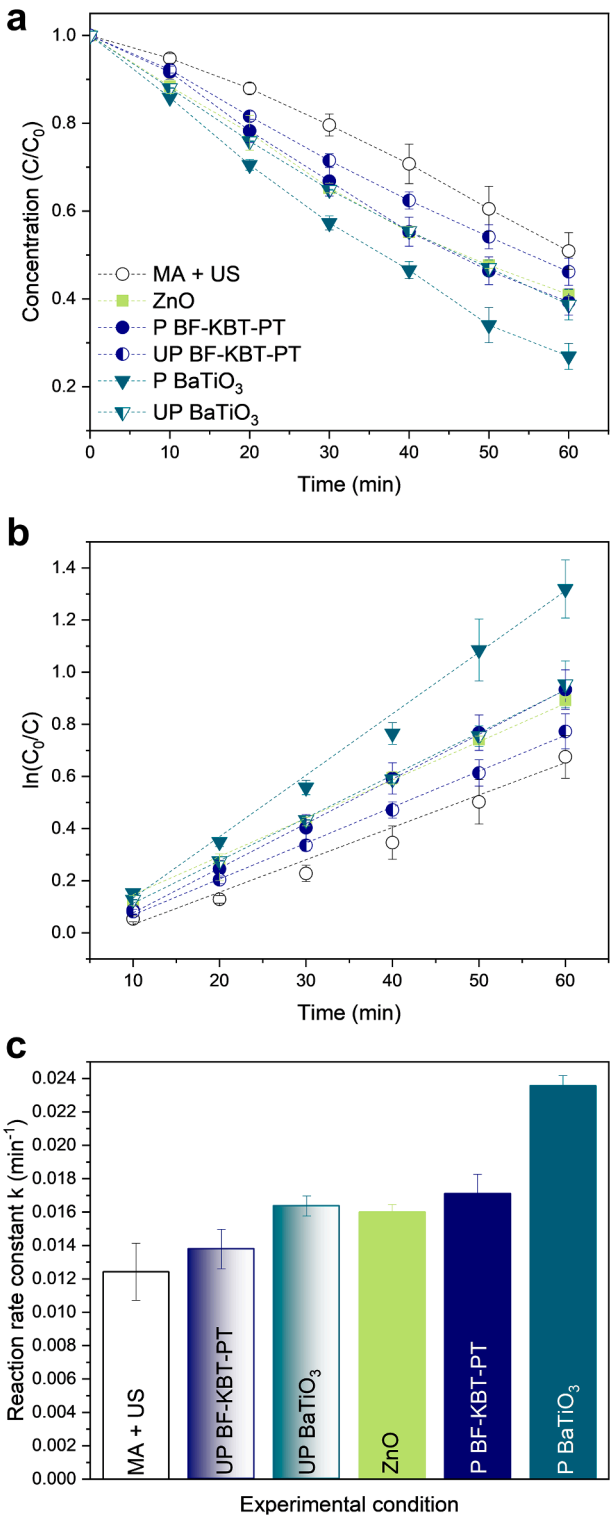

Fig. 6. RhB degradation experiments under combined ultrasound and mechanical agitation in absence and presence of piezoelectric ZnO, BF-KBT-PT and $BaTiO_3$: (a) evolution of C/C_0 vs reaction time, (b) First-order linear fit of $\ln(C_0/C)$ vs reaction time, (c) First-order degradation reaction rate constants.

electrocatalytic mechanisms (i.e. based on energy band theory and the screening charge effect) are likely to occur simultaneously. The results for ZnO further strengthens this latter idea, as a rather disappointing relative improvement of 18% was achieved in comparison to sonochemistry on its own (DE = 59%). As discussed in the previous section, ZnO piezo-electrocatalysts should generate superoxide and hydroxyl radicals both piezo-electrocatalytically and sonocatalytically. However, their poor piezoelectric nature would significantly reduce the piezo-electrocatalytical performance, even though both energy band and screening charge effect mechanisms are likely to occur.

The results agree with the hypothesis and discussion previously made in Section 3.2, strongly suggesting that both energy band and screening charge effect mechanisms are likely to occur simultaneously in piezo-electrocatalysis. To benefit from this, piezo-electrocatalysts must exhibit suitable energy band levels with a large enough band gap, as well as high piezoelectric properties (i.e. P $BaTiO_3$ piezo-electrocatalysts). A piezoelectric material that presents either one feature (i.e. suitable energy band levels with large band gap but poor piezoelectric properties like the ZnO piezoelectricatalysts) or the other (i.e. highly piezoelectric nature but small band gap like the P BF-KBT-PT piezo-electrocatalysts) may still drive redox reactions via piezo-electrocatalysis at its surface; however, its performance will be significantly lower.

This preliminary study sheds some light onto the 'true' mechanisms behind piezo-electrocatalysis, which will be extremely helpful in the future development of this research area. However, there are still many questions that need answering. For example, in the case of unpoled materials whose piezo-electric nature is mostly non-existent, RhB degradation was still occurring. The assumption is that the localised piezoelectric response at the domain level is responsible for this, but micro- and nano- piezoelectricity is a field still in its infancy, which means that more work is required to better understand this phenomenon. Furthermore, UP $BaTiO_3$ piezo-electrocatalysts worked significantly better than the UP BF-KBT-PT ones; in fact, they appeared to perform slightly better than the ZnO piezo-electrocatalysts. A potential reason for this could be that, for the reactions of interest in this study (e.g. generation of superoxide and hydroxyl radicals to degrade RhB), the overpotential required at the surface of $BaTiO_3$ may be significantly lower than that at the surface of BF-KBT-PT or ZnO. The authors are currently exploring this, although more work is required to respond to this question due to the challenging task of transferring traditional electroanalytical techniques into this area. This would enable the design of suitable piezo-electrocatalysts for more 'established' electrochemical processes such as water electrolysis [66–68] or CO_2 electroreduction [69,70], accounting not just for the piezoelectric aspect, but also for the electrochemical one.

4. Conclusion

The present study sheds more light on the 'true' mechanisms behind piezo-electrocatalysis. P $BaTiO_3$ piezo-electrocatalysts that were likely to generate superoxide and hydroxyl radicals via the two proposed mechanisms, either energy band theory or screening charge effect, were shown to deliver the largest overall degradation of RhB. This indicates that research should move from the debate on whether one mechanism *or* the other is behind piezo-electrocatalysis, to the more likely prospect that *both* mechanisms are occurring simultaneously, according to the results from this preliminary study. This opens a new opportunity in the development of piezo-electrocatalysts for different applications, where special attention must be paid to the piezoelectric nature of the materials used, as well as their energy band levels.

Besides piezo-electrocatalysis, other phenomena such as sonochemistry and (potentially) sonocatalysis were taking place during the experiments, which means that the contribution towards the overall process via their corresponding mechanisms should never be discarded in this field. Accounting for non-piezoelectricity-related mechanisms is still not usual in piezo-electrocatalysis research as previously discussed by the authors [23,25,27] and recently highlighted by other research groups [71,72]. It is hoped the results from this research will further contribute to change this perception.

CRediT authorship contribution statement

Franziska Bößl: Conceptualization, Methodology, Validation, Formal analysis, Investigation, Data curation, Writing – original draft, Visualization. **Valentin C. Menzel:** Methodology, Validation. **Karina Jeronimo:** Methodology, Resources. **Ayushi Arora:** Investigation. **Yishu Zhang:** Investigation. **Tim P. Comyn:** Resources, Writing – review & editing. **Peter Cowin:** Resources. **Caroline Kirk:** Investigation, Resources, Writing – review & editing. **Neil Robertson:** Resources, Writing – review & editing. **Ignacio Tudela:** Conceptualization, Methodology, Resources, Writing – review & editing, Supervision, Project administration, Funding acquisition.

Declaration of Competing Interest

The authors declare that they have no known competing financial interests or personal relationships that could have appeared to influence the work reported in this paper.

Data availability

Data will be made available on request.

Acknowledgements

FB and IT acknowledge the University of Edinburgh for funding this research through its Start Up fund. The authors acknowledge the use of the Zeiss Crossbeam 550 FIB-SEM funded with EPSRC grant EP/P030564/1, and would like to thank Dr Thomas Glenn and Dr Fraser Laidlaw at the University of Edinburgh for their kind support in FIB-SEM analysis. The authors would also like to thank Dr Stephen Francis at the University of St Andrews for his support with XPS analysis.

References

[1] J. Wu, Q. Xu, E. Lin, B. Yuan, N. Qin, S.K. Thatikonda, D. Bao, Insights into the role of ferroelectric polarization in piezocatalysis of nanocrystalline $BaTiO_3$, ACS Appl. Mater. Interfaces 10 (21) (2018) 17842–17849, https://doi.org/10.1021/acsami.8b01991.

[2] K. Wang, C. Han, J. Li, J. Qiu, J. Sunarso, S. Liu, The mechanism of piezocatalysis: energy band theory or screening charge effect? Angew. Chem. Int. Ed. Engl. 61 (6) (2022), e202110429 https://doi.org/10.1002/anie.202110429.

[3] H. You, Z. Wu, L. Zhang, Y. Ying, Y. Liu, L. Fei, X. Chen, Y. Jia, Y. Wang, F. Wang, S. Ju, J. Qiao, C.H. Lam, H. Huang, Harvesting the vibration energy of $BiFeO_3$ nanosheets for hydrogen evolution, Angew. Chem. Int. Ed. Engl. 58 (34) (2019) 11779–11784, https://doi.org/10.1002/anie.201906181.

[4] E. Lin, Z. Kang, J. Wu, R. Huang, N. Qin, D. Bao, $BaTiO_3$ nanocubes/cuboids with selectively deposited Ag nanoparticles: efficient piezocatalytic degradation and mechanism, Appl. Catal. B 285 (2021), https://doi.org/10.1016/j.apcatb.2020.119823.

[5] J. Wang, Y. Liang, Z. Wang, B. Huo, C. Liu, X. Chen, H. Xu, D. Li, Z. Zhu, Y. Wang, F. Meng, High efficiently degradation of organic pollutants via low-speed water flow activation of Cu2O@MoS2/PVDF modified pipeline with piezocatalysis performance, Chem. Eng. J. 458 (2023), https://doi.org/10.1016/j.cej.2023.141409.

[6] S.L. Guo, S.N. Lai, J.M. Wu, Strain-induced ferroelectric heterostructure catalysts of hydrogen production through piezophototronic and piezoelectrocatalytic system, ACS Nano 15 (10) (2021) 16106–16117, https://doi.org/10.1021/acsnano.1c04774.

[7] Y.T. Lin, S.N. Lai, J.M. Wu, Simultaneous piezoelectrocatalytic hydrogen-evolution and degradation of water pollutants by quartz microrods@few-layered mos_2 hierarchical heterostructures, Adv. Mater. 32 (34) (2020), e2002875, https://doi.org/10.1002/adma.202002875.

[8] N. Liu, R. Wang, S. Gao, R. Zhang, F. Fan, Y. Ma, X. Luo, D. Ding, W. Wu, High-performance piezo-electrocatalytic sensing of ascorbic acid with nanostructured wurtzite zinc oxide, Adv. Mater. 33 (51) (2021), e2105697, https://doi.org/10.1002/adma.202105697.

[9] J. Ma, S. Jing, Y. Wang, X. Liu, L.Y. Gan, C. Wang, J.Y. Dai, X. Han, X. Zhou, Piezo-electrocatalysis for CO_2 reduction driven by vibration, Adv. Energy Mater. 12 (27) (2022), https://doi.org/10.1002/aenm.202200253.

[10] X. Xiong, Y. Wang, J. Ma, Y. He, J. Huang, Y. Feng, C. Ban, L.Y. Gan, X. Zhou, Oxygen vacancy engineering of zinc oxide for boosting piezo-electrocatalytic hydrogen evolution, Appl. Surf. Sci. 616 (2023), https://doi.org/10.1016/j.apsusc.2023.156556.

[11] X. Ning, A. Hao, Y. Cao, N. lv, D. Jia, Boosting piezocatalytic performance of Ag decorated ZnO by piezo-electrochemical synergistic coupling strategy, Appl. Surf. Sci. 566 (2021), https://doi.org/10.1016/j.apsusc.2021.150730.

[12] H. You, Y. Jia, Z. Wu, X. Xu, W. Qian, Y. Xia, M. Ismail, Strong piezo-electrochemical effect of multiferroic BiFeO3 square micro-sheets for mechanocatalysis, Electrochem. Commun. 79 (2017) 55–58, https://doi.org/10.1016/j.elecom.2017.04.017.

[13] K.S. Hong, H. Xu, H. Konishi, X. Li, Piezoelectrochemical effect: a new mechanism for azo dye decolorization in aqueous solution through vibrating piezoelectric microfibers, J. Phys. Chem. C 116 (24) (2012) 13045–13051, https://doi.org/10.1021/jp211455z.

[14] K.S. Hong, H. Xu, H. Konishi, X. Li, Direct water splitting through vibrating piezoelectric microfibers in water, J. Phys. Chem. Lett. 1 (6) (2010) 997–1002, https://doi.org/10.1021/jz100027t.

[15] M.B. Starr, X. Wang, Coupling of piezoelectric effect with electrochemical processes, Nano Energy 14 (2015) 296–311, https://doi.org/10.1016/j.nanoen.2015.01.035.

[16] W. Qian, W. Yang, Y. Zhang, C.R. Bowen, Y. Yang, Piezoelectric materials for controlling electro-chemical processes, Nanomicro Lett. 12 (1) (2020) 149, https://doi.org/10.1007/s40820-020-00489-z.

[17] P. Wang, X. Li, S. Fan, X. Chen, M. Qin, D. Long, M.O. Tadé, S. Liu, Impact of oxygen vacancy occupancy on piezo-catalytic activity of $BaTiO_3$ nanobelt, Appl. Catal. B 279 (2020), https://doi.org/10.1016/j.apcatb.2020.119340.

[18] S. Lan, Y. Chen, L. Zeng, H. Ji, W. Liu, M. Zhu, Piezo-activation of peroxymonosulfate for benzothiazole removal in water, J. Hazard. Mater. 393 (2020), 122448, https://doi.org/10.1016/j.jhazmat.2020.122448.

[19] W. Qian, K. Zhao, D. Zhang, C.R. Bowen, Y. Wang, Y. Yang, Piezoelectric material-polymer composite porous foam for efficient dye degradation via the piezo-catalytic effect, ACS Appl. Mater. Interfaces 11 (31) (2019) 27862–27869, https://doi.org/10.1021/acsami.9b07857.

[20] G. Singh, M. Sharma, R. Vaish, Exploring the piezocatalytic dye degradation capability of lithium niobate, Adv. Powder Technol. 31 (4) (2020) 1771–1775, https://doi.org/10.1016/j.apt.2020.01.031.

[21] N. Alfryyan, S. Kumar, S.B. Ahmed, I. Kebaili, I. Boukhris, P. Azad, M.S. Al-Buriahi, R. Vaish, Electric poling effect on piezocatalytic $BaTiO_3$/polymer composites for coatings, Catalysts 12 (10) (2022), https://doi.org/10.3390/catal12101228.

[22] Q. Zhou, N. Li, D. Chen, Q. Xu, H. Li, J. He, J. Lu, Efficient removal of Bisphenol A in water via piezocatalytic degradation by equivalent-vanadium-doped SrTiO3 nanofibers, Chem. Eng. Sci. 247 (2022), https://doi.org/10.1016/j.ces.2021.116707.

[23] F. Bößl, I. Tudela, Piezocatalysis: can catalysts really dance? Curr. Opin. Green Sustain. Chem. 32 (2021) https://doi.org/10.1016/j.cogsc.2021.100537.

[24] K.P. Singh, G. Singh, R. Vaish, Utilizing the localized surface piezoelectricity of centrosymmetric Sr1-xFexTiO3 ($x \leq 0.2$) ceramics for piezocatalytic dye degradation, J. Eur. Ceram. Soc. 41 (1) (2021) 326–334, https://doi.org/10.1016/j.jeurceramsoc.2020.08.064.

[25] F. Bößl, V.C. Menzel, E. Chatzisymeon, T.P. Comyn, P.I. Cowin, I. Tudela, Effect of frequency and power on the piezocatalytic and sonochemical degradation of dyes in water, Chem. Eng. J. Adv. (2023), https://doi.org/10.1016/j.ceja.2023.100477.

[26] P.T. Thuy Phuong, Y. Zhang, N. Gathercole, H. Khanbareh, N.P. Hoang Duy, X. Zhou, D. Zhang, K. Zhou, S. Dunn, C. Bowen, Demonstration of enhanced piezo-catalysis for hydrogen generation and water treatment at the ferroelectric curie temperature, iScience 23 (5) (2020), 101095, https://doi.org/10.1016/j.isci.2020.101095.

[27] F. Bößl, T.P. Comyn, P.I. Cowin, F.R. García-García, I. Tudela, Piezocatalytic degradation of pollutants in water: importance of catalyst size, poling and excitation mode, Chem. Eng. J. Adv. 7 (2021), https://doi.org/10.1016/j.ceja.2021.100133.

[28] J. Zhang, C. Wang, C. Bowen, Piezoelectric effects and electromechanical theories at the nanoscale, Nanoscale 6 (22) (2014) 13314–13327, https://doi.org/10.1039/c4nr03756a.

[29] P. Zhu, Y. Chen, J. Shi, Piezocatalytic tumor therapy by ultrasound-triggered and $BaTiO_3$ -mediated piezoelectricity, Adv. Mater. 32 (29) (2020), e2001976, https://doi.org/10.1002/adma.202001976.

[30] A. Zhang, Z. Liu, B. Xie, J. Lu, K. Guo, S. Ke, L. Shu, H. Fan, Vibration catalysis of eco-friendly $Na_{0.5}K_{0.5}NbO_3$-based piezoelectric: an efficient phase boundary catalyst, Appl. Catal. B 279 (2020), https://doi.org/10.1016/j.apcatb.2020.119353.

[31] J. Wu, N. Qin, D. Bao, Effective enhancement of piezocatalytic activity of $BaTiO_3$ nanowires under ultrasonic vibration, Nano Energy 45 (2018) 44–51, https://doi.org/10.1016/j.nanoen.2017.12.034.

[32] V. Srikant, D.R. Clarke, On the optical band gap of zinc oxide, J. Appl. Phys. 83 (10) (1998) 5447–5451, https://doi.org/10.1063/1.367375.

[33] R. Anandhi, R. Mohan, K. Swaminathan, K. Ravichandran, Influence of aging time of the starting solution on the physical properties of fluorine doped zinc oxide films deposited by a simplified spray pyrolysis technique, Superlattices Microstruct. 51 (5) (2012) 680–689, https://doi.org/10.1016/j.spmi.2012.02.006.

[34] Y. Natsume, H. Sakata, T. Hirayama, Low-temperature electrical conductivity and optical absorption edge of ZnO films prepared by chemical vapour deposition, Phys. Status Solidi (A) 148 (2) (1995) 485–495, https://doi.org/10.1002/pssa.2211480217.

[35] M.P. Bole, D.S. Patil, Effect of annealing temperature on the optical constants of zinc oxide films, J. Phys. Chem. Solids 70 (2) (2009) 466–471, https://doi.org/10.1016/j.jpcs.2008.12.001.

[36] E. Broitman, M.Y. Soomro, J. Lu, M. Willander, L. Hultman, Nanoscale piezoelectric response of ZnO nanowires measured using a nanoindentation

technique, Phys. Chem. Chem. Phys. 15 (26) (2013) 11113–11118, https://doi.org/10.1039/c3cp50915j.
[37] T. Abu Ali, J. Pilz, P. Schäffner, M. Kratzer, C. Teichert, B. Stadlober, A.M. Coclite, Piezoelectric properties of zinc oxide thin films grown by plasma-enhanced atomic layer deposition, Phys. Status Solidi (A) 217 (21) (2020), https://doi.org/10.1002/pssa.202000319.
[38] K. Jeronimo, V. Koutsos, R. Cheung, E. Mastropaolo, PDMS-ZnO piezoelectric nanocomposites for pressure sensors, Sensors 21 (17) (2021), https://doi.org/10.3390/s21175873 (Basel).
[39] J. Bennett, A.J. Bell, T.J. Stevenson, T.P. Comyn, Tailoring the structure and piezoelectric properties of $BiFeO_3$-$K_{0.5}Bi_{0.5}TiO_3$-$PbTiO_3$ ceramics for high temperature applications, Appl. Phys. Lett. 103 (15) (2013), https://doi.org/10.1063/1.4824652.
[40] T. Stevenson, D.G. Martin, P.I. Cowin, A. Blumfield, A.J. Bell, T.P. Comyn, P. M. Weaver, Piezoelectric materials for high temperature transducers and actuators, J. Mater. Sci. Mater. Electron. 26 (12) (2015) 9256–9267, https://doi.org/10.1007/s10854-015-3629-4.
[41] H. Fan, H. Li, B. Liu, Y. Lu, T. Xie, D. Wang, Photoinduced charge transfer properties and photocatalytic activity in Bi_2O_3/$BaTiO_3$ composite photocatalyst, ACS Appl. Mater. Interfaces 4 (9) (2012) 4853–4857, https://doi.org/10.1021/am301199v.
[42] S. Das, S. Ghara, P. Mahadevan, A. Sundaresan, J. Gopalakrishnan, D.D. Sarma, Designing a lower band gap bulk ferroelectric material with a sizable polarization at room temperature, ACS Energy Lett. 3 (5) (2018) 1176–1182, https://doi.org/10.1021/acsenergylett.8b00492.
[43] H. Takahashi, Y. Numamoto, J. Tani, S. Tsurekawa, Piezoelectric properties of $BaTiO_3$ ceramics with high performance fabricated by microwave sintering, Jpn. J. Appl. Phys. 45 (9B) (2006) 7405–7408, https://doi.org/10.1143/jjap.45.7405.
[44] P. Zheng, J.L. Zhang, Y.Q. Tan, C.L. Wang, Grain-size effects on dielectric and piezoelectric properties of poled $BaTiO_3$ ceramics, Acta Mater. 60 (13–14) (2012) 5022–5030, https://doi.org/10.1016/j.actamat.2012.06.015.
[45] IEEE standard on piezoelectricity, 176–1987, 1988.
[46] IEEE standard for relaxor-based single crystals for transducer and actuator applications, 1859–2017, 2017.
[47] R.F. Contamine, A.M. Wilhelm, J. Berlan, H. Delmas, Power measurement in sonochemistry, Ultrason. Sonochem. 2 (1) (1995) S43–S47, https://doi.org/10.1016/1350-4177(94)00010-p.
[48] Y. Mao, S. Mao, Z.G. Ye, Z. Xie, L. Zheng, Solvothermal synthesis and Curie temperature of monodispersed barium titanate nanoparticles, Mater. Chem. Phys. 124 (2–3) (2010) 1232–1238, https://doi.org/10.1016/j.matchemphys.2010.08.063.
[49] S. Trasatti, The absolute electrode potential: an explanatory note (Recommendations 1986), Pure Appl. Chem. 58 (7) (1986) 955–966, https://doi.org/10.1351/pac198658070955.
[50] V.K. Sharma, Oxidation of inorganic contaminants by ferrates (VI, V, and IV)–kinetics and mechanisms: a review, J. Environ. Manag. 92 (4) (2011) 1051–1073, https://doi.org/10.1016/j.jenvman.2010.11.026.
[51] W.H. Koppenol, D.M. Stanbury, P.L. Bounds, Electrode potentials of partially reduced oxygen species, from dioxygen to water, Free Radic. Biol. Med. 49 (3) (2010) 317–322, https://doi.org/10.1016/j.freeradbiomed.2010.04.011.
[52] M.C. Blanco López, B. Rand, F.L. Riley, The isoelectric point of BaTiO3, J. Eur. Ceram. Soc. 20 (2) (2000) 107–118, https://doi.org/10.1016/s0955-2219(99)00137-5.
[53] F. Yuan, H. Peng, Y. Yin, Y. Chunlei, H. Ryu, Preparation of zinc oxide nanoparticles coated with homogeneous Al_2O_3 layer, Mater. Sci. Eng. B 122 (1) (2005) 55–60, https://doi.org/10.1016/j.mseb.2005.04.016.
[54] M.A. Abbasi, A. Rehman, Z. Ali, M. Atif, Z. Ali, W. Khalid, Congo red removal by lanthanum-doped bismuth ferrite nanostructures, J. Phys. Chem. Solids 170 (2022), https://doi.org/10.1016/j.jpcs.2022.110964.
[55] J. Moon, J.A. Kerchner, J. LeBleu, A.A. Morrone, J.H. Adair, Oriented lead titanate film growth at lower temperatures by the sol-gel method on particle-seeded substrates, J. Am. Ceram. Soc. 80 (10) (2005) 2613–2623, https://doi.org/10.1111/j.1151-2916.1997.tb03164.x.
[56] Y. Wang, X. Wen, Y. Jia, M. Huang, F. Wang, X. Zhang, Y. Bai, G. Yuan, Y. Wang, Piezo-catalysis for nondestructive tooth whitening, Nat. Commun. 11 (1) (2020) 1328, https://doi.org/10.1038/s41467-020-15015-3.
[57] O. Copie, N. Chevalier, G. Le Rhun, C.L. Rountree, D. Martinotti, S. Gonzalez, C. Mathieu, O. Renault, N. Barrett, Adsorbate screening of surface charge of microscopic ferroelectric domains in sol-gel $PbZr_{0.2}Ti_{0.8}O_3$ thin films, ACS Appl. Mater. Interfaces 9 (34) (2017) 29311–29317, https://doi.org/10.1021/acsami.7b08925.
[58] P. Qiu, B. Park, J. Choi, B. Thokchom, A.B. Pandit, J. Khim, A review on heterogeneous sonocatalyst for treatment of organic pollutants in aqueous phase based on catalytic mechanism, Ultrason. Sonochem. 45 (2018) 29–49, https://doi.org/10.1016/j.ultsonch.2018.03.003.
[59] S. Chakma, V.S. Moholkar, Investigation in mechanistic issues of sonocatalysis and sonophotocatalysis using pure and doped photocatalysts, Ultrason. Sonochem. 22 (2015) 287–299, https://doi.org/10.1016/j.ultsonch.2014.06.008.
[60] F. Peng, H. Li, W. Xu, H. Min, Z. Li, F. Li, X. Huang, W. Wang, C. Lu, A discovery of field-controlling selective adsorption for micro ZnO rods with unexpected piezoelectric catalytic performance, Appl. Surf. Sci. 545 (2021), https://doi.org/10.1016/j.apsusc.2021.149032.
[61] Y. Bai, J. Zhao, Z. Lv, K. Lu, Enhanced piezocatalytic performance of ZnO nanosheet microspheres by enriching the surface oxygen vacancies, J. Mater. Sci. 55 (29) (2020) 14112–14124, https://doi.org/10.1007/s10853-020-05053-z.
[62] C. Yu, M. Tan, Y. Li, C. Liu, R. Yin, H. Meng, Y. Su, L. Qiao, Y. Bai, Ultrahigh piezocatalytic capability in eco-friendly $BaTiO_3$ nanosheets promoted by 2D morphology engineering, J. Colloid Interface Sci. 596 (2021) 288–296, https://doi.org/10.1016/j.jcis.2021.03.040.
[63] D. Liu, C. Jin, F. Shan, J. He, F. Wang, Synthesizing $BaTiO_3$ nanostructures to explore morphological influence, kinetics, and mechanism of piezocatalytic dye degradation, ACS Appl. Mater. Interfaces 12 (15) (2020) 17443–17451, https://doi.org/10.1021/acsami.9b23351.
[64] X. Xu, Z. Wu, L. Xiao, Y. Jia, J. Ma, F. Wang, L. Wang, M. Wang, H. Huang, Strong piezo-electro-chemical effect of piezoelectric BaTiO3 nanofibers for vibration-catalysis, J. Alloy. Compd. 762 (2018) 915–921, https://doi.org/10.1016/j.jallcom.2018.05.279.
[65] J. González-García, V. Sáez, I. Tudela, M.I. Díez-Garcia, M. Deseada Esclapez, O. Louisnard, Sonochemical treatment of water polluted by chlorinated organocompounds. A review, Water 2 (1) (2010) 28–74, https://doi.org/10.3390/w2010028.
[66] Y. Long, H. Xu, J. He, C. Li, M. Zhu, Piezoelectric polarization of BiOCl via capturing mechanical energy for catalytic H_2 evolution, Surf. Interfaces 31 (2022), https://doi.org/10.1016/j.surfin.2022.102056.
[67] J. He, Z. Yi, Q. Chen, Z. Li, J. Hu, M. Zhu, Harvesting mechanical energy induces piezoelectric polarization of MIL-100(Fe) for cocatalyst-free hydrogen production, Chem. Commun. (Camb.) 58 (76) (2022) 10723–10726, https://doi.org/10.1039/d2cc03976a.
[68] Y. Zhang, H. Khanbareh, S. Dunn, C.R. Bowen, H. Gong, N.P.H. Duy, P.T. T. Phuong, High efficiency water splitting using ultrasound coupled to a $BaTiO_3$ nanofluid, Adv Sci (Weinh.) 9 (9) (2022), e2105248, https://doi.org/10.1002/advs.202105248.
[69] J. He, X. Wang, S. Lan, H. Tao, X. Luo, Y. Zhou, M. Zhu, Breaking the intrinsic activity barriers of perovskite oxides photocatalysts for catalytic CO_2 reduction via piezoelectric polarization, Appl. Catal. B 317 (2022), https://doi.org/10.1016/j.apcatb.2022.121747.
[70] P.T.T. Phuong, D.V.N. Vo, N.P.H. Duy, H. Pearce, Z.M. Tsikriteas, E. Roake, C. Bowen, H. Khanbareh, Piezoelectric catalysis for efficient reduction of CO_2 using lead-free ferroelectric particulates, Nano Energy 95 (2022), https://doi.org/10.1016/j.nanoen.2022.107032.
[71] H. Kalhori, A.H. Youssef, A. Ruediger, A. Pignolet, Competing contributions to the catalytic activity of barium titanate nanoparticles in the decomposition of organic pollutants, J. Environ. Chem. Eng. 10 (6) (2022), https://doi.org/10.1016/j.jece.2022.108571.
[72] M.M. Amer, R. Hommelsheim, C. Schumacher, D. Kong, C. Bolm, Electro-mechanochemical approach towards the chloro sulfoximidations of allenes under solvent-free conditions in a ball mill, Farady Discuss. 241 (0) (2023) 79–90, https://doi.org/10.1039/d2fd00075j.